ORIGINAL PAPER

Can the positive aromatic ring be as π-electron donor in π-halogen bond? A MP2 theoretical investigation on the unusual π-halogen bond interaction between three-membered ring $(BNN)_3^+$ and X1X2 (X1, X2=F, Cl, Br)

Hai-tao Qi · Fu-de Ren · Jing-lin Zhang · Jing-yu Wang

Abstract The unusual π-halogen bond interactions are investigated between $(BNN)_3^+$ and X1X2 (X1, X2=F, Cl, Br) employing MP2 at 6-311+G(2d) and aug-cc-pVDZ levels according to the "CP (counterpoise) corrected potential energy surface (PES)" method. The order of the π-halogen bond interactions and stabilities of the complexes are obtained to be $(BNN)_3^+ \ldots F_2 < (BNN)_3^+ \ldots$ ClF $< (BNN)_3^+ \ldots Cl_2 < (BNN)_3^+ \ldots BrCl < (BNN)_3^+ \ldots$ $Br_2 < (BNN)_3^+ \ldots BrF.$ at MP2/aug-cc-pVDZ level. The analyses of the Mulliken charge transfer, natural bond orbital (NBO), atoms in molecules (AIM) theory and electron density shifts reveal that the nature of the π-halogen bond interaction in the complexes of ClF, BrF and BrCl might partly be charge transfer from the delocalized π-HOMO orbital of $(BNN)_3^+$ to X1X2. This result suggests that the positive aromatic ring $(BNN)_3^+$ might act as a π-electron donor to form the π-halogen bond.

Keywords $(BNN)_3^+ \cdot$ Electron density shifts $\cdot$ MP2 $\cdot$ π-electron donor $\cdot$ π-halogen bond interaction

Introduction

Recently π-halogen bond interactions have received much attention in experimental and theoretical investigations as a result of their extremely important roles in a wide range of biological and chemical fields including crystal engineer-

ing, new supramolecular structures, drug design, etc. [1–21]. In particular, they are often involved in protein-ligand interactions of the aromatic amino acids [22–24]. Furthermore, in most cases, the π-halogen bonded complexes are key intermediates in the electrophilic halogenations of alkenes, alkynes, allenes and aromatic systems [13, 14, 19]. It has been shown that these kind of interactions can be established between the electron-rich aromatic rings (including ringed anions) as π-electron donors, and dihalogens as well as organic halides [13]. Then, can the electron-deficient aromatic ring (for example, positive aromatic ring) be as π-electron donor to form the π-halogen bond? In general it is difficult. However, it is well known that the π-electrons have strong fluidity. Thus for the model $R^+ \ldots X1–X2$ (R^+: positive aromatic ring with π-electron), if the ability of electron withdrawing of the X1X2 group from R^+ is strong enough, and at the same time, π-electron of R^+ is easy enough to be released, R^+ will become a π-electron donor and the unusual π-halogen bond will be formed. In fact, the search for the new and "unusual" complex in chemical bonding has long been a primary goal in molecular modeling.

Interestingly, very recently we have found that, although the BB multiple-bond is the electron-deficient group, the π-electron is easy to be released to form the π-hydrogen bond and cation-π interaction [25–31]. Therefore, we turned our attention to the simplest and positive three-membered aromatic ring $(BNN)_3^+$ containing the BB multiple-bond. $(BNN)_3^+$ is of D_{3h} symmetry and it has been predicted to be most aromatic among the planar monocyclic boron nitrides [32]. In this species, each boron atom is of normal sp^2 hybridization to connect with a coordinating N_2 ligand and two adjacent B atoms, leaving one p_z atom orbital out

H.-t. Qi · F.-d. Ren (✉) · J.-l. Zhang · J.-y. Wang
College of Chemical Engineering and Environment,
North University of China,
Taiyuan 030051, China
e-mail: renfude@hotmail.com

of plane to take part in the delocalized π-HOMO orbital. Thus a three-centered two-electron (3c-2e) delocalized π-bond comes into being [32]. Since the π-electron of the BB multiple-bond is easy to be released and two π-electrons are just at HOMO orbital for $(BNN)_3^+$, $(BNN)_3^+$ is considered a candidate to model the π-halogen bonded complex in which the positive aromatic ring is the π-electron donor.

In 2003, the π-halogen bonded complexes formed as essential intermediates from alkenes, alkynes, and allenes with bromine were investigated by UV-spectroscopy in combination with stopped-flow techniques. Calculations by *ab initio* method reproduced the experimentally determined thermodynamic values quite well [14]. In 2005, Li et al. studied the π-halogen bonds of ClF with ethylene and its derivatives at MP2/aug-cc-pVDZ level, showing that the stabilities of the π-halogen bond systems resulted primarily from the dispersion interaction [7]. In 2007, an *ab initio* calculation carried out to investigate the interactions between the π face of benzene and several halocarbon molecules, indicating that the C–X/π interactions were comparable in strength to the C–H/π interactions [3]. Very recently, an advance on halogen bonding has been reviewed [33]. All the previous investigations paid close attention to the π-halogen interactions containing only the electron-rich π-electron donors. However, to our knowledge, no investigation on the π-halogen bond involving the electron-deficient positive aromatic ring as the π-electron donor has been presented.

In this paper, our goal is to test whether the electron-deficient positive aromatic three-membered ring $(BNN)_3^+$ can be as the π-electron donor to form π-halogen interaction with X1X2 (X1, X2=F, Cl, Br) or not. For this kind of novel π-halogen interactions, theoretic investigation will reveal the nature of the interaction to further study on structures and activities for the complexes involving the positive and electron-deficient aromatic species as π-electron donors in theory and experiment.

Computational methods

It is well established that, employing MP2 method with the augmented correlation-consistent polarized valence-double-ζ (aug-cc-pVDZ) basis set, the π-halogen bond interaction compares relatively well to the experimental value, and thus the MP2/aug-cc-PVDZ method has been successfully applied in order to understand the nature of the π-halogen bond interaction [3, 7, 34]. Therefore, MP2/aug-cc-pVDZ is used in this investigation. As a comparison, MP2/6-311+G(2d) is also considered.

All the calculations have been performed using Gaussian 03 programs [35]. All the possible π-halogen interaction complexes have been fully optimized using MP2 with the 6-311+G(2d) and aug-cc-pVDZ basis sets according to the

"CP-corrected PES)" method [36, 37]. We have also performed the "standard PES (i.e., non-counterpoise (NCP))" geometrical optimization. The complexes corresponding to the minimum energy points, at which the harmonic frequency analyses have been carried out, at the molecular energy hypersurface have been obtained. At present, based on the *ab initio* optimized structure, natural bond orbital (NBO) analysis [38] with Gaussian 03 program packages is being applied widely to gain insights into the origin of halogen bonding interactions [39–44]. Therefore, NBO analysis has been carried out at MP2/aug-cc-pVDZ level. The shifts of the electron densities [45] that accompany the formation of the π-halogen bonds have been displayed at MP2/aug-cc-pVDZ level using Gauss-View program and the topological electron charge density has been analyzed by the AIM method [46] using AIMPAC program [47] at the same level. The frequency shifts (Δν), defined as the difference between the frequency of the certain vibrational mode in the complex and isolated X1X2, can be expressed as follows:

$$\Delta v = v_{\text{com.}} - v_{\text{mono.}} \tag{1}$$

Binding energy (D_e) is expressed as follows:

$$D_e = -\left(E_{\left((BNN)_3^+ - X1X2\right)\text{com.}} - E_{(BNN)_3^+\text{mono.}} - E_{X1X2\,\text{mono.}} \right). \tag{2}$$

The D_e corrected for the basis set superposition error (BSSE) [36, 37] is evaluated.

Results and discussion

The structure and π-HOMO orbital of $(BNN)_3^+$ are illustrated in Fig. 1. The atomic labels and bond critical points (BCPs) of the complexes are shown in Fig. 2. The geometry parameters, Mulliken charges in the X1X2 moiety and electron densities at the BCPs are listed in Table 1. The binding energies are collected in Table 2.
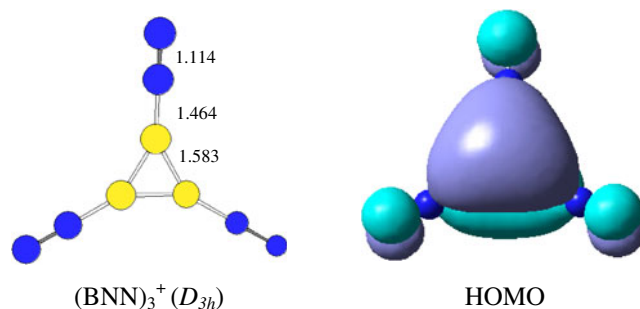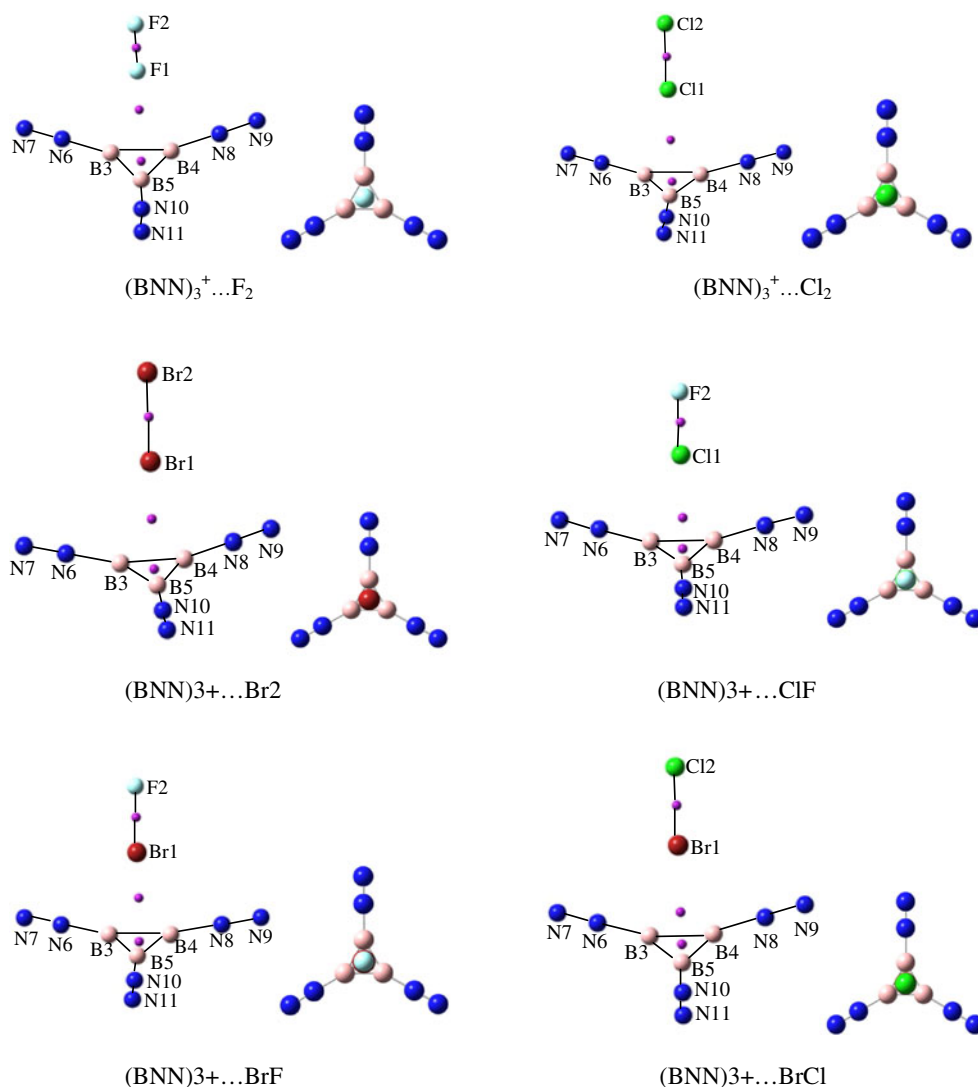

Fig. 1 Optimized structure and π molecular orbital (HOMO) of aromatic planar monocyclic at MP2/aug-cc-PVDZ level

Fig. 2 Molecular structures, bond critical points of the complexes at MP2/aug-cc-pVDZ level

(BNN)$_3^+$...F$_2$

(BNN)$_3^+$...Cl$_2$

(BNN)3+...Br2

(BNN)3+...ClF

(BNN)3+...BrF

(BNN)3+...BrCl

Frequency shifts and NBO analysis are given in Tables 3 and 4, respectively.

All of the investigations on the complexes in which the dihalogen with dipole moments approaches $(BNN)_3^+$ with the F atom for FCl and FBr as well as with the Cl atom for ClBr are in vain. In these complexes, the π-electrons are not released from $(BNN)_3^+$. On the other hand, for the complexes in which the halogen points toward boron or the midpoint of the BB bonds, we have found that they are not energetically preferable in comparison with the complexes in which the halogen points toward the centroid of the ring. Therefore, $(BNN)_3^+ \ldots FCl$, $(BNN)_3^+ \ldots FBr$ and $(BNN)_3^+ \ldots ClBr$ as well as the complexes in which the halogen points toward boron or the midpoint of the BB bonds are not considered in this paper. It is noted that, in π-HOMO of $(BNN)_3^+$, the most of the π-electron densities lie in the centroid of the ring (it is not the case in C_6H_6) (see Fig. 1), suggesting that π-electron might transfer the most in C_{3V} symmetry

complexes. Thus, only six C_{3V} shaped complexes are obtained.

Geometry of the complex

From Table 1, the π-halogen bond length R(X1…π) (the distance between the centroid of the $(BNN)_3^+$ ring and X1) from the CP-corrected PES method is always longer by about 0.1 Å than that from the standard PES, as is similar to the investigation on the H-bonded and π-halogen bonded systems by Li et al. [7, 48]. However, the X1–X2 bond length R(X1–X2) from CP-corrected PES is very close to that from the standard PES, and the difference is no more than 0.01 Å.

For $(BNN)_3^+ \ldots F_2$, $(BNN)_3^+ \ldots Cl_2$ and $(BNN)_3^+ \ldots Br_2$, the increments of the X1–X2 bond lengths are increased by 0.012, 0.015 and 0.021 Å using the CP-corrected PES method at MP2/aug-cc-PVDZ level, respectively. Furthermore, the π-halogen bond lengths R(X1…π) are 2.852,

Table 1 Principal geometry parameters (in Å), Mulliken charges Q (in me) and bond critical point properties (in au) for the monomers (R(X1–X2)$_{mono.}$) and π-halogen bonded complexes (BNN)$_3^+$...X1X2[a]

parameters	(BNN)$_3^+$...F$_2$	(BNN)$_3^+$...Cl$_2$	(BNN)$_3^+$...Br$_2$	(BNN)$_3^+$...ClF	(BNN)$_3^+$...BrF	(BNN)$_3^+$...BrCl
R(X1...π)	2.774 [b] 2.659 [c]	2.857 2.870	2.833 2.816	2.534 2.594	2.475 2.474	2.787 2.755
	2.963 [b] 2.852 [c]	**3.030 3.043**	**3.018 3.026**	**2.724 2.753**	**2.629 2.610**	**2.968 2.952**
R(X1–X2)	1.424 1.449	2.047 2.063	2.362 2.359	1.706 1.709	1.808 1.841	2.205 2.216
	1.418 1.439	**2.042 2.054**	**2.356 2.345**	**1.685 1.695**	**1.818 1.825**	**2.193 2.200**
R(X1–X2)$_{mono.}$	1.410 1.427	2.029 2.039	2.335 2.324	1.665 1.677	1.786 1.793	2.176 2.180
QX1 [c]	34.07	32.73	25.50	280.46	292.42	157.58
QX2 [c]	–19.04	–20.30	–24.62	–412.51	–492.52	–192.62
Q$_{X1X2}$ [c]	15.03	12.43	0.88	–132.05	–200.10	–35.04
$\rho_{BCP(X...\pi)}$ [c]	0.0106	0.0131	0.0159	0.0479	0.0329	0.0180
$\nabla^2\rho_{BCP(X...\pi)}$ [c]	0.0397	0.0410	0.0452	0.0320	0.0717	0.0498
$\rho_{BCP(X1–X2)}$ [c]	0.2598	0.1428	0.1000	0.2463	0.1396	0.1171
$\nabla^2\rho_{BCP(X1–X2)}$ [c]	0.3977	–0.0891	–0.0290	0.3649	0.2566	–0.0354
$\rho_{RCP(B3–B4–B5)}$ [c]	0.1285	0.1282	0.1280	0.0424	0.1267	0.1278
$\nabla^2\rho_{RCP(B3–B4–B5)}$ [c]	0.0956	0.1012	0.1018	0.1389	0.1081	0.1036

[a] The values in bold are obtained by the CP-corrected PES method

[b] At MP2/6-311+G(2d) level

[c] At MP2/aug-cc-PVDZ level

3.043 and 3.026 Å, respectively, falling below the sum of the van der Waals radii of the halogen and boron atoms. Thus, the halogen-bonded interactions in (BNN)$_3^+$...F$_2$, (BNN)$_3^+$...Cl$_2$ and (BNN)$_3^+$...Br$_2$ are suggested.

The halogen-bonded interactions in the (BNN)$_3^+$ complexes of ClF, BrF and BrCl are also found according to the increments of the X1–X2 bond lengths and the short X1...π distances. The increments of the X1–X2 bond lengths are increased by 0.018, 0.032 and 0.020 Å, and X1...π bond distances are only 2.753, 2.610 and 2.952 Å, respectively.

As can be seen from Table 1, the distance of the X1...π bond is the same order of (BNN)$_3^+$...Cl$_2$>(BNN)$_3^+$...Br$_2$ >, (BNN)$_3^+$...F$_2$ and (BNN)$_3^+$...BrCl >(BNN)$_3^+$...ClF >(BNN)$_3^+$...BrF using four methods, and the increments of the X1–X2 bond length are (BNN)$_3^+$...F$_2$ <

(BNN)$_3^+$...Cl$_2$ <(BNN)$_3^+$...Br$_2$ and (BNN)$_3^+$...ClF < (BNN)$_3^+$...BrCl < (BNN)$_3^+$...BrF. These results suggest that the strength of the halogen-bonded interaction in (BNN)$_3^+$...BrF might be the greatest.

Binding energies and stabilities

As can be seen from Table 2, for the interaction energies from NCP optimized geometries, the proportion of correlated interaction energies to their total binding energies, defined as $[(-D_e)-(-D_{e(BSSE/ZPE)})]/(-D_e)$, are up to 59.82 and 55.79 % at MP2/6-311+G(2d) and MP2/aug-cc-pVDZ levels for BSSE corrections, respectively. In our previous investigations on the cation-π interactions, the proportions are up to 5.53 and 11.93 % at MP2(full)/6-311++G(2df, 2p)

Table 2 Binding energies of the π-halogen bonded complexes (D_e (kJ mol^{-1})) and electron correlation (EC) effect value $\left(EC = D_{e, MP2/6-311+G(2d)} - D_{e, HF/6-311+G(2d)}\right)$ [a]

	(BNN)$_3^+$...F$_2$	(BNN)$_3^+$...Cl$_2$	(BNN)$_3^+$...Br$_2$	(BNN)$_3^+$...ClF	(BNN)$_3^+$...BrF	(BNN)$_3^+$...BrCl
MP2/6-311+G(2d)	13.14 (5.28)	26.73 (13.85)	36.68 (19.13)	23.88 (9.85)	35.89 (17.67)	33.46 (16.08)
	6.01	**15.25**	**21.12**	**11.97**	**20.67**	**17.91**
MP2/aug-cc-pVDZ	14.66 (6.70)	26.77 (14.69)	39.88 (18.88)	24.42 (10.51)	42.68 (19.56)	37.14 (16.42)
	7.72	**16.14**	**21.36**	**12.14**	**22.30**	**18.68**
HF/6-311+G(2d)	**0.39**	**0.61**	**0.77**	**–5.79**	**–7.27**	**–2.09**
EC	**5.62 (93.5 %)**	**14.64 (96.0 %)**	**20.35 (96.4 %)**	**17.76 (148.4 %)**	**27.94 (135.2 %)**	**20.00 (111.7%)**

[a] The values (in plain) in the parentheses is BSSE-corrected ($-D_{e(BSSE)}$). The values in plain are obtained by the standard PES method, and those in bold are obtained by the CP-corrected PES method

Table 3 Selected frequency shifts relative to the monomers for the complexes at MP2/aug-cc-pVDZ [a]

	$(BNN)_3^+\dots F_2$		$(BNN)_3^+\dots Cl_2$		$(BNN)_3^+\dots Br_2$		$(BNN)_3^+\dots ClF$		$(BNN)_3^+\dots BrF$		$(BNN)_3^+\dots BrCl$		Assignment [b]
	$\nu/\Delta\nu$	I	$\nu/\Delta\nu$	I	$\nu/\Delta\nu$	I	$\nu/\Delta\nu$	I	$\nu/\Delta\nu$	I	$\nu/\Delta\nu$	I	
ν_1	92	0	99	0	98	0	107	2	112	2	101	1	stret. of X1...π [c]
ν_2	–1	0	–3	0	–7	1	–7	0	–14	6	–8	2	sym. stret. of B–B [d]
ν_3	3	148	1	138	–2	132	–5	111	–13	97	–4	123	anti-sym. stret. of B–B [e]
ν_4	–65	14 (0) [f]	–35	6 (0)	–25	6 (0)	–87	144 (22)	–84	163 (27)	–41	37 (1)	stret. of X1–X2

[a] All frequencies (ν or $\Delta\nu$) are in cm^{-1} and IR intensities (I) are in km/mol.

[b] Stret. stands for stretching, and sym. means symmetrical.

[c] For the intermolecular bond stretching frequencies of the six complexes, the reduced masses are 12.36, 12.68, 12.35, 13.07, 13.30 and 12.58 AMU, and the force constants are 0.061, 0.074, 0.070, 0.089, 0.098 and 0.075 mD/Å, respectively.

[d] The symmetrical stretching of the B–B bond in the isolated $(BNN)_3^+$ monomer is 1458 cm-1, and the corresponding IR intensity is 0 km/mol.

[e] The anti-symmetrical stretching of the B–B bond in the isolated $(BNN)_3^+$ monomer is 1070 cm-1, and the corresponding IR intensity is 147 km/mol.

[f] he values in the parentheses are IR intensities for isolated X1X2 monomers and their frequencies are 934, 538, 316, 781, 681 and 432 cm-1 respectively, and the values out of the parentheses are those for the monomers in the complexes.

and MP2(full)/aug-cc-pVTZ, respectively [27]. For the X–H...π hydrogen-bonded interactions, they are up to 16.93 and 15.98 % at MP2/6-311++G(2df, 2p) and MP2/aug-cc-pVTZ levels, respectively [28]. Clearly, the effect of BSSE on the π-halogen bond interaction is larger than that on the cation-π or π-hydrogen bond interaction, as is in good agreement with the investigation by Li et al. (about 57 % for the halogen bond interactions at UMP2/aug-cc-pVDZ level) [49]. These results indicate that it is very necessary for the π-halogen bond interaction energies to check the BSSE corrections. Therefore, in this investigation we have performed the CP-corrected PES geometrical optimization

and, as follows in the discussion, the accurate structures from the CP-corrected PES are used.

The calculated results show that the MP2/aug-cc-pVDZ energy difference [D_e (CP) $-(D_e$ (NCP, BSSE))] between CP and NCP geometries is as follows: 1.12 (13.2%), 1.45 (9.0%), 2.48 (11.6%), 1.63 (13.4%), 2.74 (12.3%) and 2.26 (12.1%) for the $(BNN)_3^+$ complexes of F$_2$, Cl$_2$, Br$_2$, ClF, BrF and BrCl, respectively. The result shows that the interaction from CP is stronger than that from NCP geometry, as is in agreement with the study on the π-halogen interactions in complexes $C_2H_{4-n}F_n\dots ClF$ (n=0-2) [7]. Moreover, we have found that the interaction energies

Table 4 Calculated NBO parameters of complexes at their equilibrium geometries: NBO occupation numbers for the B atoms with lone pairs or B–B bonds (Occ.(LpB) or Occ.(B–B)), the (X1–X2)* antibonds (Occ.(X1–X2)*), their respective orbital energies ε, the second-order perturbation energies $E^{(2)}$ and the NBO charge transfer of the monomers X1X2 in their complexes (Q) at MP2/aug-cc-pVDZ

	$(BNN)_3^+\dots F_2$	$(BNN)_3^+\dots Cl_2$	$(BNN)_3^+\dots Br_2$	$(BNN)_3^+\dots ClF$	$(BNN)_3^+\dots BrF$	$(BNN)_3^+\dots BrCl$
Occ.(LpB)[a]	0.6290 p$^{1.00}$	0.6297 p$^{1.00}$	0.6283 p$^{1.00}$	0.6259 p$^{1.00}$	0.6190 p$^{1.00}$	0.6280 p$^{1.00}$
ε\{(LpB) \}[b]	–0.0820	–0.0859	–0.0894	–0.0980	–0.1088	–0.0940
Occ.(X1–X2)* [a]	0.0090 sp$^{18.53}$ sp$^{20.57}$	0.0214 sp$^{13.90}$ sp$^{15.29}$	0.0394 sp$^{19.19}$ sp$^{19.38}$	0.0632 sp$^{20.88}$sp$^{9.11}$	0.1450 sp$^{30.09}$ sp$^{7.72}$	0.0502 sp$^{20.48}$ sp$^{14.11}$
ε\{(X1–X2)\}* [b]	–0.0048	–0.0143	–0.0652	0.0108	–0.0267	–0.0441
$E^{(2)}$ $_{(LpB)\rightarrow\sigma(X1-X2)^*}$ [c]	7.65	17.61	85.10	40.73	142.94	58.30
Occ.(B–B)[a]		1.8247 sp$^{1.71}$ sp$^{1.71}$	1.8262 sp$^{1.70}$ sp$^{1.70}$	1.8295 sp$^{1.70}$ sp$^{1.70}$	1.8333 sp$^{1.71}$ sp$^{1.71}$	1.8278 sp$^{1.70}$ sp$^{1.70}$
ε\{(B–B)\}[b]		–0.6748	–0.6779	–0.6883	–0.6999	–0.6828
$E^{(2)}$ $_{\sigma(B-B)\rightarrow\sigma(X1-X2)^*}$ [c]		0.25	0.96	2.17	9.12	1.46
Q(X1X2)[d]	–2.9	0.2	–4.3	–24.5	–47.6	–9.19

[a] Occ.: occupation number,

[b] In a.u.,

[c] In kJ/mol,

[d] In me.

calculated at MP2/aug-cc-pVDZ level are higher than those from MP2/6-311+G(2d). The previous investigations showed that the results at the MP2/aug-cc-pVDZ level were more reliable [3, 7].

At the MP2/aug-cc-pVDZ level, the order of the π-halogen bond interaction and stability of the complex are obtained as $(BNN)_3^+ \dots F_2 < (BNN)_3^+ \dots ClF < (BNN)_3^+ \dots Cl_2 < (BNN)_3^+ \dots BrCl < (BNN)_3^+ \dots Br_2 < (BNN)_3^+ \dots BrF$. Two effects on the π-halogen bond interaction strength have been taken into consideration. We address, first, the effect of the polarization of the X1 atom. As is well known that the polarization is enhanced in the order F<Cl< Br, and therefore, the binding energies obtained are in the order of $(BNN)_3^+ \dots F_2 < (BNN)_3^+ \dots Cl_2 < (BNN)_3^+ \dots Br_2$ and $(BNN)_3^+ \dots ClF < (BNN)_3^+ \dots BrF$, as is in agreement with the order of the increments of the X1–X2 bond length, while it is the reverse of the trend in the intermolecular distances X1…π. Second, the effect of the electron withdrawing of the X2 atom is mentioned. In general, the more electron-withdrawing ability of the group bound to the halogen X1, the shorter the intermolecular separation will become, and the stronger the π-halogen bond interaction will form. Lu et al. have found that this tendency appears to be simply interpreted by the electrostatic character of the π-halogen bond interactions since electron-withdrawing groups enhance the positive electrostatic potential of halogen atoms X1 [3]. Thus, the binding energies submit to the order of $(BNN)_3^+ \dots BrCl < (BNN)_3^+ \dots BrF$ and $(BNN)_3^+ \dots ClF < (BNN)_3^+ \dots Cl_2$. Of course, the dipole moment of the dihalogen plays an important role in relative stabilities of the complexes of ClF, BrF and BrCl. At MP2/aug-cc-pVDZ level, the dipole moments of them are 1.2875, 1.8008 and 0.5777 D, respectively, suggesting that the π-halogen bond interaction in $(BNN)_3^+ \dots BrF$ is the strongest, too.

Moreover, electron correlation has a pronounced effect on the calculated interaction energies. Indeed, the significant attraction by electron correlation (the contribution is up to 93.5–148.4 %) has found. Due to the positive interaction yielded from HF, the percentage is over 100%, as is well consistent with the previous investigation on the π-halogen bond interactions [3]. Li et al. have also found that the electron correlation contribution (up to 184 %) causes the large interaction energy [7].

Mulliken charge transfer

The charges (electronegative) of moiety X1X2 can be considered as the charge transfer from $(BNN)_3^+$ to X1X2, because the charge for each isolated X1X2 is zero. Thus, the charges of the X1X2 moiety (the sum of the Mulliken charges in two halogen atoms) might be used to roughly represent electron acceptor ability of the X1X2, and

therefore indicate indirectly the electron donor ability of $(BNN)_3^+$ in complexes.

From Table 1, the negative charges of the X1X2 moiety are found in the complexes of ClF, BrF and BrCl, suggesting that charge transfer might play a role in these complexes and $(BNN)_3^+$ might be the electron donor. The order of the negative charge of the X1X2 moiety is as follows: –35.04 me (BrCl)<–132.05 me (ClF) < –200.10 me (BrF). Thus, the electron donor ability of $(BNN)_3^+$ might be in $(BNN)_3^+ \dots BrF > (BNN)_3^+ \dots ClF > (BNN)_3^+ \dots BrCl$, as is almost in accordance with the order of the π-halogen interaction.

As can also be seen from Table 1, the negativity of X2 increases in the complex of ClF, BrCl or BrF in comparison with that of the monomer and the positive charge rises for X1. Thus the X1X2 moiety becomes more polarized and the ability of electron withdrawing of the X1X2 group from R^+ turns stronger. As a result, it might lead to the charge transfer from $(BNN)_3^+$ to X1X2.

Vibration frequencies

As can be seen from Table 3, for the $(BNN)_3^+$ complexes with F_2, Cl_2, Br_2 and ClF, BrF, BrCl, the intermolecular bond X1…π stretching frequencies (ν_1) are predicted to be 92, 99, 98 and 107, 112, 101 cm^{-1} at MP2/aug-cc-pVDZ level, indicating the formation of the intermolecular interactions. These values follow the order of $(BNN)_3^+ \dots BrF > (BNN)_3^+ \dots ClF > (BNN)_3^+ \dots BrCl > (BNN)_3^+ \dots Br_2 > (BNN)_3^+ \dots Cl_2 > (BNN)_3^+ \dots F_2$, as is in agreement with the order of the binding energies except for $(BNN)_3^+ \dots ClF$ and $(BNN)_3^+ \dots BrCl$. It is noted that a certain vibrational mode is not one single vibrational frequency but a combination of many of the vibrational patterns.

The larger the frequency shifts, the more stable the complex is, so we also showed some important frequency shifts in order to investigate the relative stabilities of the complexes. The most important vibrational frequency of π-electron donor $(BNN)_3^+$, ν_2, can be approximately described as the symmetrical stretching of the B–B bond (i.e., symmetrical breathing vibration of the ring). From Table 3, it can be seen that the ν_2 decreased (red shifts) in the complexes in comparison with those of the monomers, showing the formation of the π-halogen bond interaction. Furthermore, the values of the frequency shifts follow the order of $(BNN)_3^+ \dots Brf > (BNN)_3^+ \dots BrCl > (BNN)_3^+ \dots Br_2 = (BNN)_3^+ \dots ClF > (BNN)_3^+ \dots Cl_2 > (BNN)_3^+ \dots F_2$, as is almost consistent with the order of the binding energies.

The ν_3 and ν_4 can be described as the anti-symmetrical stretching of the B–B bond (i.e., anti-symmetrical breathing vibration of the ring) and stretching frequencies of the X1–

Fig. 3 Shifts of electron density as a result of formation of the complex

$(BNN)_3^+\ldots F_2$

$(BNN)_3^+\ldots Cl_2$

$(BNN)_3^+\ldots Br_2$

$(BNN)_3^+\ldots ClF$
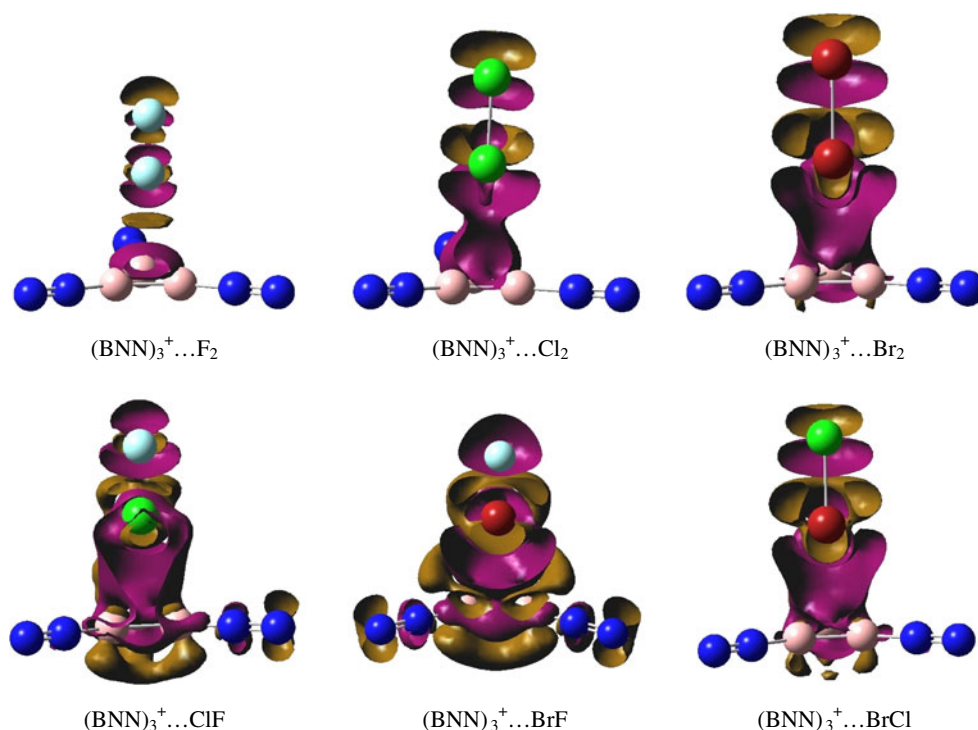
$(BNN)_3^+\ldots BrF$

$(BNN)_3^+\ldots BrCl$

X2 bond, respectively. Although the ν_3 increased for $(BNN)_3^+\ldots F_2$ and $(BNN)_3^+\ldots Cl_2$ while decreased in others, the frequencies changed more greatly in $(BNN)_3^+\ldots BrF$ than those in the other complexes, indicating that the π-halogen interaction in $(BNN)_3^+\ldots BrF$ is the strongest. The same behavior is also observed in ν_4.

NBO analysis

According to the NBO analysis, all the complexes have two units. The delocalization effects between two units can be identified from the presence of off-diagonal elements of the Fock matrix in the NBO basis, and the strengths of these delocalization interactions, $E^{(2)}$ [38], can be estimated by second-order perturbation theory. From Table 4, we can see that the major interaction is that the boron atom offers the $p^{1.00}$-hybridization electrons to the (X1–X2)* antibonding orbital. These delocalization interactions $E^{(2)}_{(LpB)\rightarrow\sigma(X1-X2)}$ have stabilized the systems by 7.65, 17.61, 85.10, 40.73, 142.94 and 58.30 kJ mol^{-1}, respectively, indicating that the orbital interaction might play a role in the halogen-bonding interaction. It should be noteworthy that, the lone pair of boron atom (LpB) is not actually the real "lone pair" but forms the 3c-2e delocalized π-orbital [32]. Indeed, the NBO occupancies of each lone pair of boron atom are about 0.62, and the total occupancies are close to two, i.e., two π-electrons. Thus, the π-halogen interactions in these complexes might be confirmed.

On the other hand, the NBO charge transfer is evaluated to be from $(BNN)_3^+$ to ClF, BrF and BrCl by –24.5, –47.6

and –9.19 me, respectively. This result shows an increase of electron density on X1X2, simultaneously a decrease of electron density on $(BNN)_3^+$, suggesting that $(BNN)_3^+$ is the electron-donor and charge transfer might play an important role in π-halogen interactions, as is in accordance with the previous investigations [14, 18, 20, 49]. Furthermore, we have also noted the fact that the net charge transfers from the complexes with F_2, Cl_2 and Br_2 are always less than those from the complexes with ClF, BrF and BrCl. This is due to the weaker polarization of the former than that of the latter. The net charge transfer in $(BNN)_3^+\ldots BrF$ is the largest, suggesting that the interaction in $(BNN)_3^+\ldots BrF$ is the strongest, too.

AIM analysis

It is well known that the electronic characteristics are very essential to reveal the nature of the intermolecular interactions. As an advanced method, AIM of Bader [46] has been applied widely to study the π-halogen bond interactions [3, 49]. In this theory, the nuclei act as point attractors immersed in a cloud of negative charge, the electron density $\rho(r)$. The special point where $\Delta\rho(r)$ (the gradient vector) vanishes is called critical point, which are denoted as (ω, σ) (the ω is equal to the number of non-zero eigenvalues or non-zero curvature of $\rho(r)$ at the critical point, and the σ is the algebraic sum of signs of eigenvalues). The (3, –1) and (3, +1) are saddle points, called the bond critical point (BCP) and the ring critical point (RCP) respectively.

Our calculated AIM results show that, for each $X1...\pi$ contact, there is a bond path linking the halogen atom $X1$ with one boron atom of $(BNN)_3^+$, accompanied by a BCP (see Fig. 2), as is similar to the investigation on the halocarbon–benzene complex by Lu et al. [3]. Their calculated AIM results also show that, for each of the $C–X/\pi$ contacts, a bond path linking the halogen atom accompanied by a BCP is found. Furthermore, for all the complexes $(BNN)_3^+...X1X2$, the values of the electron densities $\rho_{BCP(X1...\pi)}$ obtained are within a range of 0.0106 – 0.0479 a.u. (see Table 1), which just fall into the common accepted values for intermolecular interactions (0.002–0.04 a.u.). Moreover, the values of their Laplacians $\nabla^2\rho_{BCP}$ are all positive, indicating the typical closed-shell kind of interactions in the complexes. In other words, for these $X1...\pi$ contacts, the small ρ_{BCP} and positive $\nabla^2\rho_{BCP}$ values are basically similar to the topological properties of normal π-halogen bonds [3, 49]. This result suggests again the formation of π-halogen bond interaction and confirms that, the positive aromatic ring $(BNN)_3^+$ might be as π-electron donors to form the π-halogen bond interactions.

As also can be seen From Table 1, the electron density at the ring critical point ($\rho_{RCP(B3–B4–B5)}$) follows the order of $(BNN)_3^+...ClF < (BNN)_3^+...BrF < (BNN)_3^+...BrCl < (BNN)_3^+...Br_2 < (BNN)_3^+...Cl_2 < (BNN)_3^+...F_2$, suggesting that the order of electron donor ability of $(BNN)_3^+...ClF > (BNN)_3^+...BrF > (BNN)_3^+...BrCl > (BNN)_3^+...Br_2 > (BNN)_3^+...Cl_2 > (BNN)_3^+...F_2$, as is almost in accordance with the order of the π-halogen interactions except for $(BNN)_3^+...ClF$ and $(BNN)_3^+...Br_2$.

Analysis of the electron density shifts

To clarify further the nature of the π-halogen bond interaction between $(BNN)_3^+$ and $X1X2$ in detail, the analysis of the electron density shifts that accompany formation of the π-halogen interaction has been carried out. The shifts of electron densities are illustrated in Fig. 3. This map is generated by comparing the density in the complexes, point by point in space, to the same quantity in the isolated monomers. Purple regions hence represent the accumulation of additional electron density as a result of the mutual approach of the two molecules; yellow regions indicate loss of density.

The obvious effects of the halogen-bond formation for the complexes of F_2, Cl_2 and Br_2 are shown by the purple upbow-region above the plane containing the boron and nitrogen atoms, consistent with the accepted notion that the positive aromatic ring accumulates density from $X1X2$.

Different from the complexes of F_2, Cl_2 and Br_2, for those of ClF, BrF and BrCl, the notable yellow region

above and below the plane containing three boron atoms is found, indicating that the π-HOMO orbital of $(BNN)_3^+$ loses density. Much of this lost density is shifted toward $X1$, indicated by the large purple between $(BNN)_3^+$ and $X1$, and little of the density loss is shifted to $(BNN)_3^+$ itself (little purple in the plane). Thus, π-halogen interaction is formed, as is in accordance with the analyses mentioned above.

Therefore, we might conclude that, although it is difficult to establish halogen-bond interaction between a positive ion and a region of positive electrostatic potential (halogen bonding involves a region of positive electrostatic potential on the outside of the halogen [50–52]), the π-HOMO orbital of $(BNN)_3^+$ tends to lose density in the complexes of ClF, BrF and BrCl due to the strong fluidity of the π-electrons and great electron withdrawing of $X1X2$. As a result, $(BNN)_3^+$ acts not as a positive ion but as a π-electron donor to interact with a region of positive electrostatic potential of $X1$ in this kind of unusual π-halogen interactions.

Conclusions

The unusual π-halogen bond interactions are investigated between $(BNN)_3^+$ and $X1X2$ ($X1$, $X2$=F, Cl, Br). The order of the π-halogen interactions and stabilities of the complexes are $(BNN)_3^+...F_2 < (BNN)_3^+...ClF < (BNN)_3^+...Cl_2 < (BNN)_3^+...BrCl < (BNN)_3^+...Br_2 < (BNN)_3^+...BrF$. The dipole moment of dihalogen, the effects of the polarization of the $X1$ atom and the electron withdrawing of the $X2$ atom influence the strength of the π-halogen bond interaction. The positive aromatic ring $(BNN)_3^+$ with the electron-deficient boron might be a π-electron donor to form the π-halogen bond.

References

1. Mazik M, Buthe AC, Jones PG (2010) Tetrahedron 66:385–389
2. Cincic D, Friscic T, Jones W (2008) Chem Eur J 14:747–753
3. Lu YX, Zou JW, Wang YH, Yu QS (2007) Chem Phys 334:1–3
4. Masu H, Mizutani I, Ono Y, Kishikawa K, Azumaya I, Yamaguchi K, Kohmoto S (2006) Cryst Growth Des 6:2086–2091
5. Bishop R, Scudder ML, Craig DC, Rahman ANMM, Alshahateet SF (2005) Mol Cryst Liq Cryst 440:173–186
6. Swierczynski D, Luboradzki R, Dolgonos G, Lipkowski J, Schneider HJ (2005) Eur J Org Chem 11:1172–1177
7. Li RY, Li ZR, Wu D, Li Y, Chen W, Sun CC (2005) J Phys Chem A 109:2608–2613
8. Forni A, Metrangolo P, Pilati T, Resnati G (2004) Cryst Growth Des 4:291–295
9. Glaser R, Chen NJ, Wu H, Knotts N, Kaupp M (2004) J Am Chem Soc 126:4412–4419
10. Adams H, Cockroft SL, Guardigli C, Hunter CA, Lawson KR, Perkins J, Spey SE, Urch CJ, Ford R (2004) Chem Bio Chem 5:657–665

11. Rahman ANMM, Bishop R, Craig DC, Scudder ML (2004) Org Biomol Chem 2:175–182
12. Rahman ANMM, Bishop R, Craig DC, Scudder ML (2003) Cryst Eng Commun 5:422–428
13. Lenoir D (2003) Angew Chem Int Ed 42:854–857
14. Lenoir D, Chiappe C (2003) Chem Eur J 9:1037–1044
15. Rahman ANMM, Bishop R, Craig DC, Scudder ML (2002) Cryst Eng Commun 4:510–513
16. Turner B, Shterenberg A, Kapon M, Suwinska K, Eichen Y (2001) Chem Commun 1:13–14
17. Bailey WR, Padgett CW, Metrangolo P, Resnati G, Hanks TW, Pennington WT (2001) Cryst Growth Des 1:165–175
18. Bianchini R, Chiappe C, Lo Moro G, Lenoir D, Lemmen P, Goldberg N (1999) Chem Eur J 5:1570–1580
19. Legon AC (1999) Angew Chem Int Ed 38:2686–2714
20. Bianchini R, Chiappe C, Lenoir D, Lemmen P, Herges R, Grunenberg J (1997) Angew Chem Ed Int Engl 36:1284–1287
21. Lommerse JPM, Stone AJ, Taylor R, Allen FH (1996) J Am Chem Soc 118:3108–3116
22. Jiang Y, Alcaraz AA, Chen JM, Kobayashi H, Lu YJ, Snyder JP (2006) J Med Chem 49:1891–1899
23. Battistutta R, Mazzorana M, Sarno S, Kazimierczuk Z, Zanotti G, Pinna LA (2005) Chem Biol 12:1211–1219
24. Metrangolo P, Neukirch H, Pilati T, Resnati G (2005) Acc Chem Res 38:386–395
25. Cao D, Ren F, Liu S, Chen S (2009) J Mol Struct Theochem 913:221–227
26. Xu W, Ren F, Ren J, Liu S, Yue Y, Wang W, Chen S (2010) J Mol Model 16:615–627
27. Wu Y, Ren F, Li B (2009) J Mol Struct Theochem 909:79–85
28. Ren F, Cao D, Wang W, Ren J, Hou S, Chen S (2009) J Mol Model 15:515–523
29. Ren F, Cao D, Wang W, Ren J, Chen S (2009) J Mol Struct Theochem 896:38–43
30. Ren F, Cao D, Wang W, Hou S, Chen S (2008) J Mol Struct Theochem 870:43–48
31. Ren F, Cao D, Wang W, Wang J, Li Y, Hu Z, Chen S (2008) Chem Phys Lett 455:32–37
32. Li QS, Xu Y (2007) J Comput Chem 28:1446–1455
33. Fourmigué M (2009) Curr Opin Solid State Mater Sci 13:36–45
34. Lu YX, Zou JW, Yu QS, Jiang YJ, Zhao WN (2007) Chem Phys Lett 449:6–10
35. Frisch MJ et al. (2003) Gaussian 03, Revision B.03. Gaussian Inc, Pittsburgh
36. Duijineveldt FB, Duijineveldt-van de Rijdt JCMV, Lenthe JHV (1994) Chem Rev 94:1873–1885
37. Boys SF, Bernardi F (1970) Mol Phys 19:553–566
38. Reed AE, Curtis LA, Weinhold FA (1988) Chem Rev 88:899–926
39. Evans CJ, Wright TG, Gardner AM (2010) J Phys Chem A 114:4446–4454
40. Wang W, Ji B, Zhang Y (2009) J Phys Chem A 113:8132–8135
41. Li Y, Wu D, Li ZR (2008) Inorg Chem 47:9773–9778
42. Wang W, Hobza P (2008) J Phys Chem A 112:4114–4119
43. Lu YX, Zou JW, Wang YH, Jiang YJ, Yu QS (2007) J Phys Chem A 111:10781–10788
44. Lin CY, Coote ML, Petit A, Richard P, Poli R, Matyjaszewski K (2007) Macromolecules 40:5985–5994
45. Scheiner S, Kar T (2002) J Phys Chem A 106:1784–1789
46. Bader RFW (1990) Atoms in Molecules, A Quantum Theory. Oxford University Press, New York
47. Bieger-Konig FW, Bader RFW, Tang TH (1982) J Comput Chem 3:317–328
48. Wu D, Li ZR, Hao XY, Jalbout AF, Adamowicz L, Li RJ, Sun CC (2004) J Chem Phys 120:1330–1335
49. Li Q, An X, Gong B, Cheng J (2008) J Mol Struct Theochem 866:11–14
50. Politzer P, Lane P, Concha MC, Ma Y, Murray JS (2007) J Mol Model 13:305–311
51. Clark T, Hennemann M, Murray JS, Politzer P (2007) J Mol Model 13:291–296
52. Politzer P, Murray JS, Lane P (2007) Int J Quant Chem 107:3046–3052